Expanded View Figures

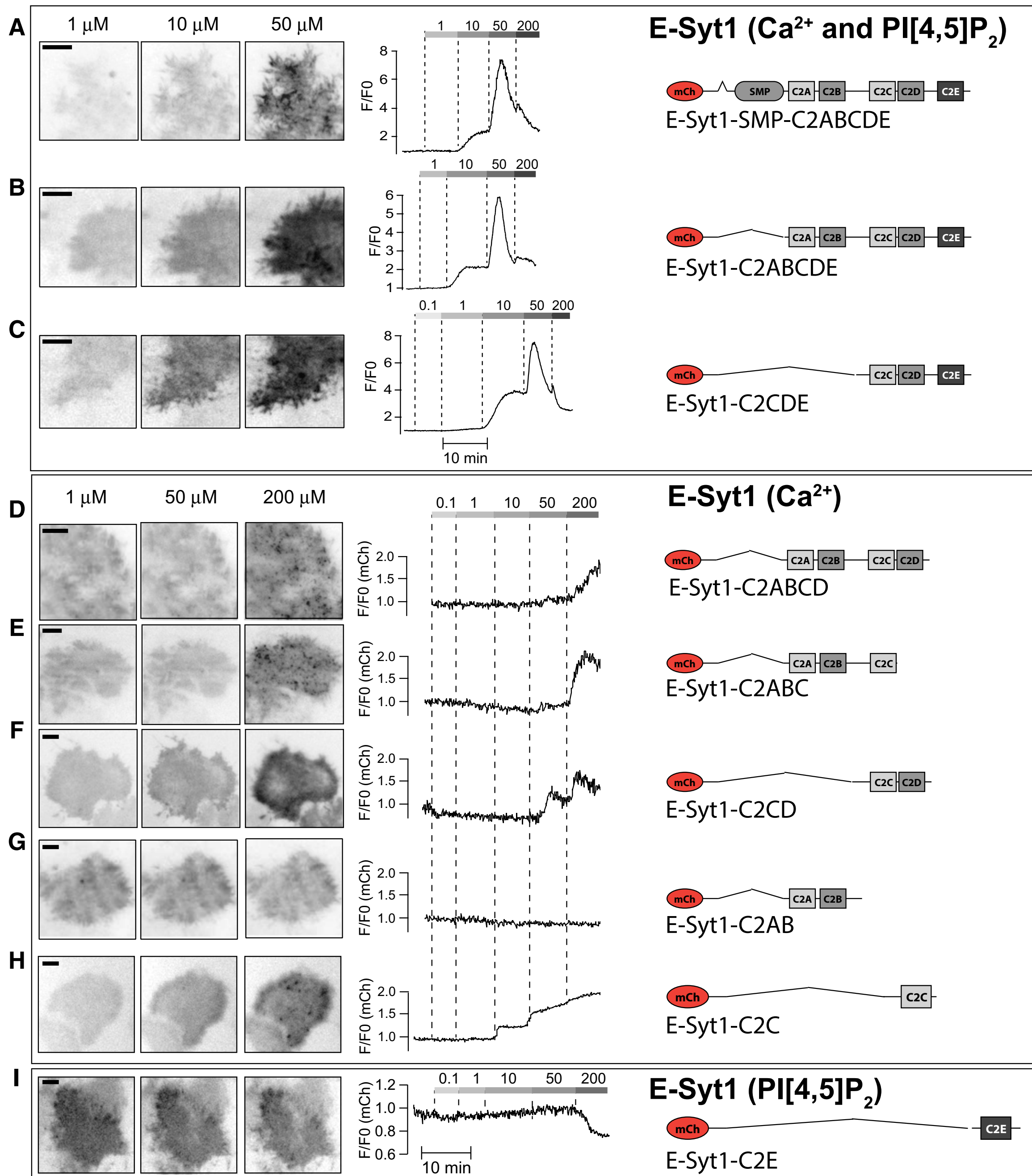

Figure EV1. Contribution of the different C2 domains to E-Syt1 plasma membrane binding (relates to Figure 2).

A–C TIRF micrographs (left) and single-cell TIRF recordings of mCherry fluorescence for the indicated E-Syt1 domain deletion protein binding the plasma membrane $PI(4,5)P_2$ in a Ca^{2+}-dependent manner.

D–H TIRF micrographs (left) and single-cell TIRF recordings of mCherry fluorescence for the indicated E-Syt1 domain deletion protein binding the plasma membrane in a $PI(4,5)P_2$-independent and Ca^{2+}-dependent manner.

I TIRF micrographs (left) and single-cell TIRF recording of mCherry fluorescence for the indicated E-Syt1 domain deletion protein binding the plasma membrane in a $PI(4,5)P_2$-dependent and Ca^{2+}-independent manner.

Data information: The clustering or aggregation of fluorescent protein seen in (D, E and H) is only observed at 200 μM Ca^{2+} and reflects cytosolic aggregates. All scale bars, 10 μm.

 © 2015 The Authors

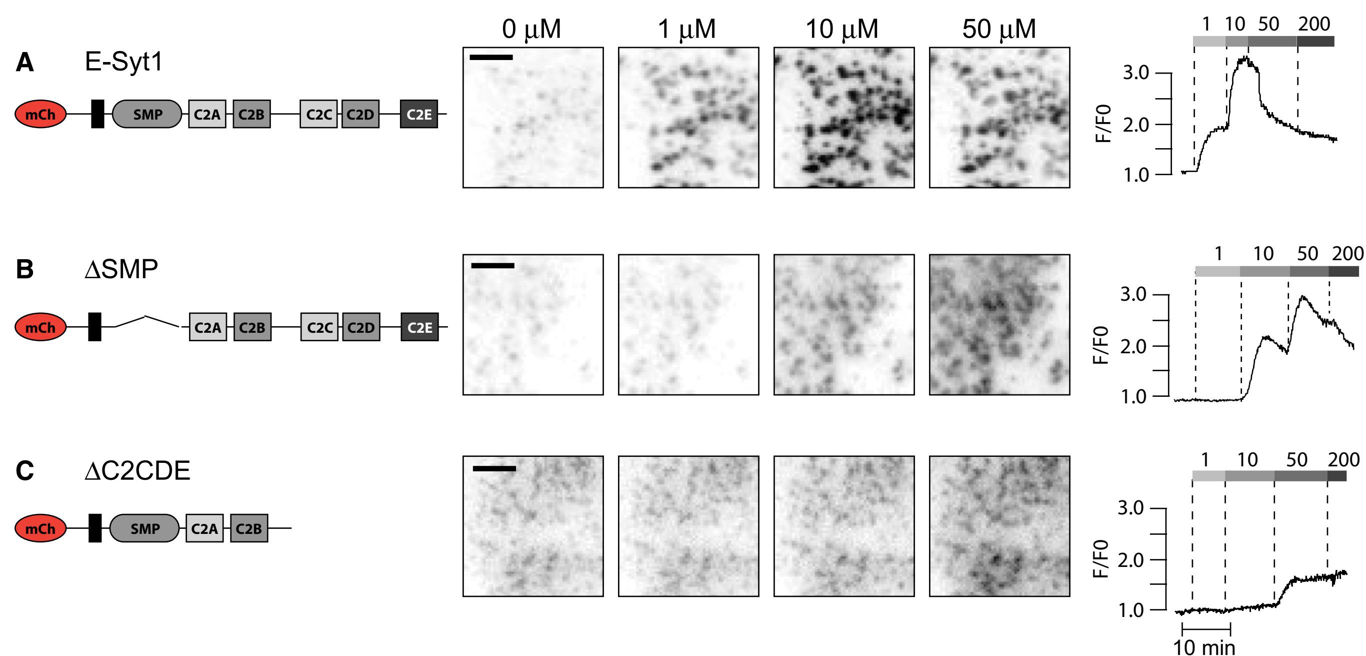

Figure EV2. Contribution of the SMP domain to E-Syt1 plasma membrane binding (relates to Figure 3).

A–C TIRF micrographs (left) and single-cell TIRF recordings of mCherry fluorescence (right) for the indicated, ER-localized E-Syt1 domain deletion proteins. All scale bars, 2 µm.

© 2015 The Authors

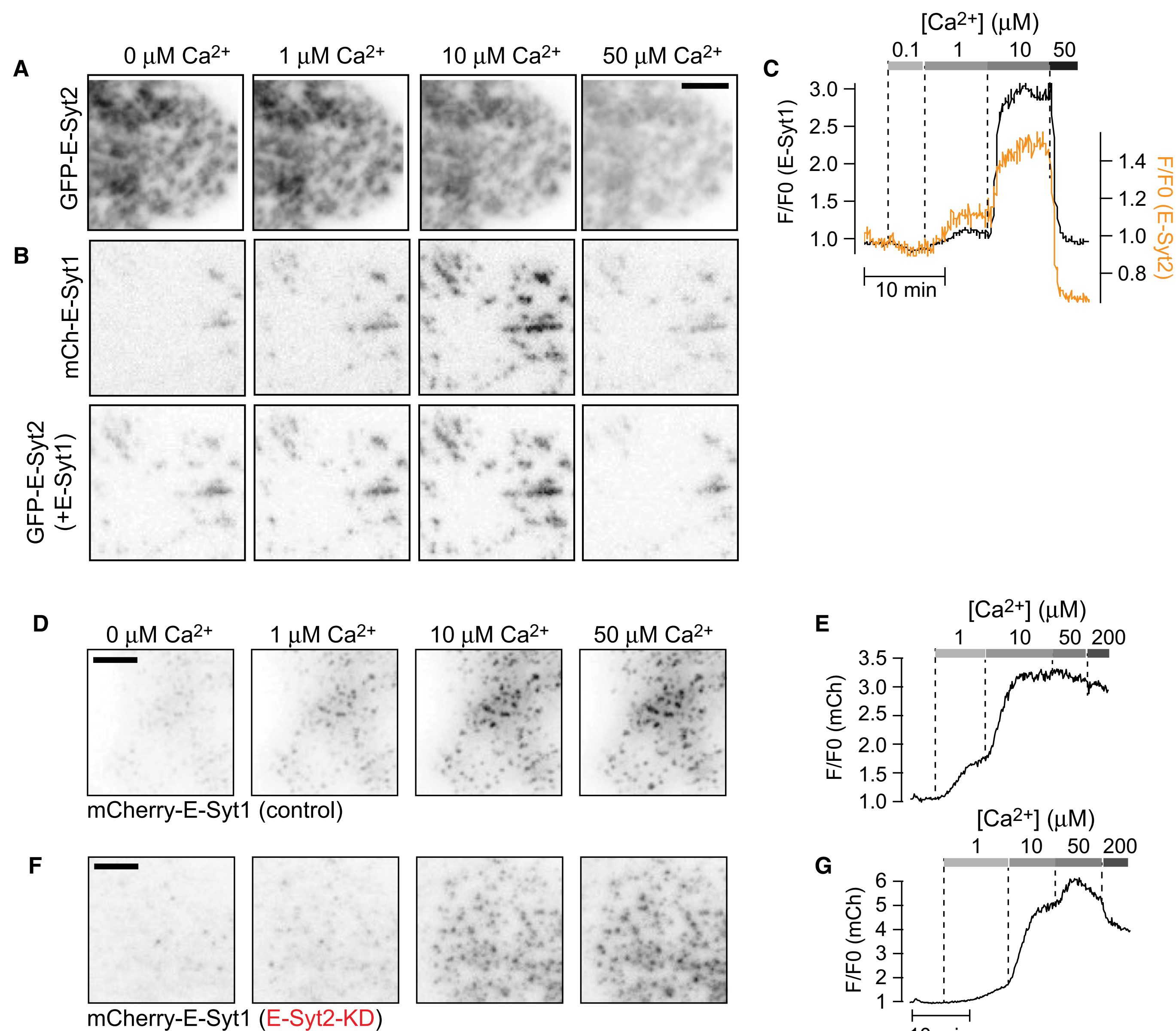

Figure EV3. E-Syt1-E-Syt2 heterodimerization has an impact on plasma membrane binding (relates to Figure 3).

A, B TIRF micrographs of GFP-E-Syt2 (A) or GFP-E-Syt2 and mCherry-E-Syt1 (B) fluorescence from a permeabilized cell exposed to buffers with the indicated Ca^{2+} concentrations.

C Single-cell TIRF recording of mCherry-E-Syt1 (black) and GFP-E-Syt2 (yellow) fluorescence following exposure to buffers with the indicated Ca^{2+} concentrations.

D, E TIRF micrographs (D) and single-cell TIRF recording (E) of mCherry-E-Syt1 fluorescence in control cells after permeabilization and exposure to buffers with the indicated Ca^{2+} concentrations.

F, G TIRF micrographs (F) and single-cell TIRF recording (G) of mCherry-E-Syt1 fluorescence in E-Syt2 knockdown cells after permeabilization and exposure to buffers with the indicated Ca^{2+} concentrations.

Data information: All scale bars, 2 µm.

 © 2015 The Authors

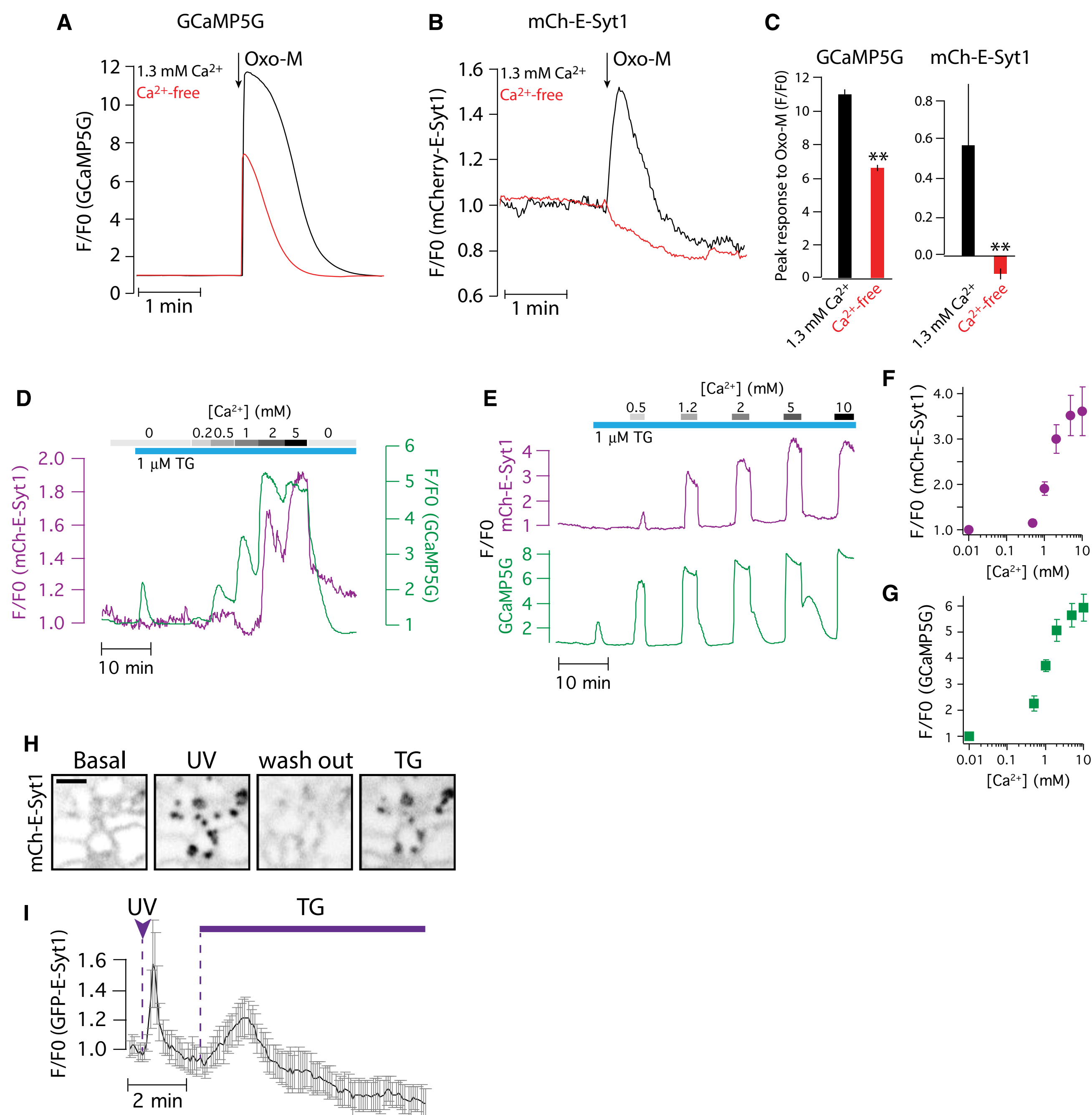

Figure EV4. E-Syt1 PM binding requires triggered Ca^{2+} influx (relates to Figure 4).

A, B TIRF microscopy recordings of GCaMP5G (A) and mCherry-E-Syt1 (B) fluorescence following stimulation with 10 μM oxo-M, in the absence (red) or presence (black) of extracellular Ca^{2+}. The HeLa cells also overexpressed an M1 muscarinic receptor.

C Quantification of the peak Ca^{2+} increase (left) and E-Syt1 PM binding (right) from the experiments in (A) and (B). Data show means ± SEM for 19 cells from 3 separate experiments (**$P < 0.01$ for difference from 1.3 mM Ca^{2+}).

D, E TIRF microscopy recordings of GCaMP5G (green) and mCherry-E-Syt1 (purple) fluorescence following exposure to 1 μM thapsigargin in the absence of extracellular Ca^{2+}, followed by the addition of Ca^{2+} at different concentrations (0.2–10 mM).

F, G Quantification of the peak fluorescence increase in mCherry-E-Syt1 (F) and GCaMP5G (G) measured by TIRF microscopy in response to the application of the indicated Ca^{2+} concentration in the presence of 1 μM thapsigargin. Data show means ± SEM for 19 cells from 4 experiments.

H Confocal micrographs of mCherry-E-Syt1 fluorescence from a HeLa cell maintained in a Ca^{2+}-containing buffer and exposed to flash photolysis of caged Ca^{2+} and subsequent addition of 1 μM thapsigargin (TG). Scale bar, 1 μm.

I Means ± SEM (n = 4 cells from 2 experiments) of mCherry-E-Syt1 fluorescence change at ER-PM contacts following flash photolysis of Ca^{2+} and subsequent addition of 1 μM thapsigargin (TG).

© 2015 The Authors

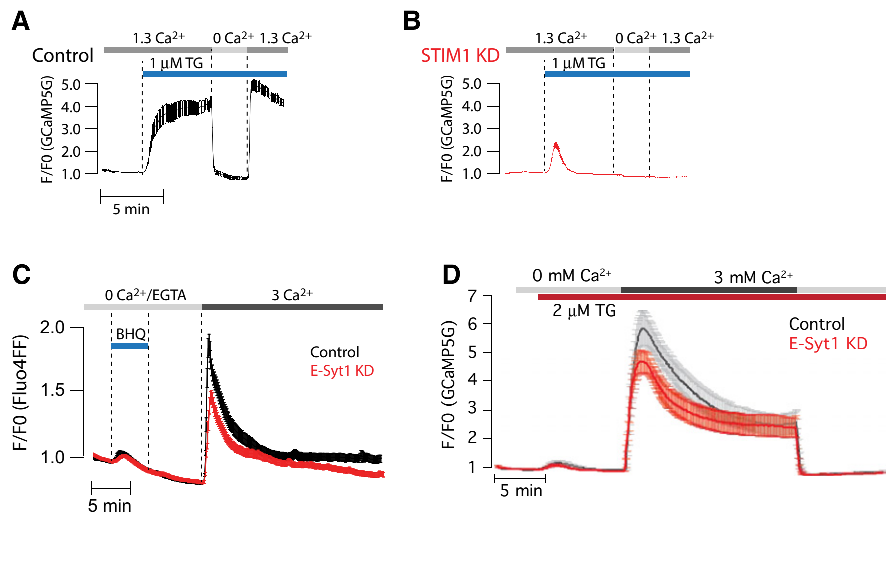

Figure EV5. E-Syt1 knockdown has little impact on SOCE (relates to Figure 4).

A, B TIRF microscopy recordings of GCaMP5G fluorescence in response to 1 µM thapsigargin (TG) in control (A, black) and STIM1 siRNA-treated (B, red) HeLa cells (means ± SEM for 31 (control) and 28 (STIM1 KD) cells in 3 separate experiments).

C Ca^{2+} imaging of control or E-Syt1 KD HeLa cells loaded with the low-affinity Ca^{2+} indicator Fluo-4FF during release of Ca^{2+} from the ER and activation of SOCE. Curves are presented as means ± SEM for 38 (control, red) and 33 (E-Syt1 KD, black) cells from 4 separate experiments.

D Fluorescence microscopy recordings of GCaMP5G fluorescence in control or E-Syt1 knockdown HeLa cells exposed to 1 µM thapsigargin (TG) in Ca^{2+}-free buffer, followed by the re-addition of 3 mM Ca^{2+}. Data are presented as means ± SEM for 21 (control) and 23 (E-Syt1-KD) cells from 3 experiments.

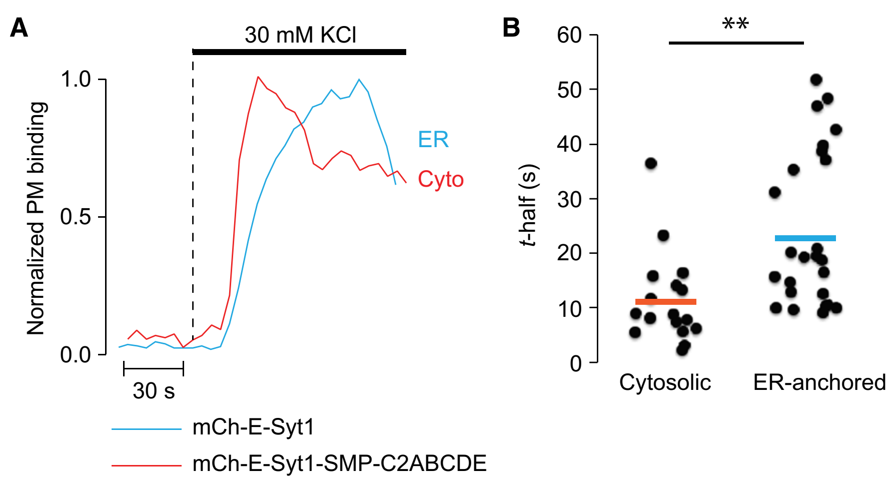

Figure EV6. Different PM-binding kinetics of cytosolic and ER-localized E-Syt1.

A Representative TIRF microscopy recordings from two MIN6 cells expressing mCherry-E-Syt1 (blue) or mCherry-E-Syt1-SMP-C2ABCDE (red) following depolarization with 30 mM K^{+}.

B Scatter plot showing time to half-maximal PM binding for cells stimulated as in (A). N = 17 cells (mCherry-E-Syt1) and N = 24 cells (mCherry-E-Syt1-SMP-C2ABCDE) from 2 separate experiments (**P < 0.01).

© 2015 The Authors